The evolution of mutation rates in the light of development and cell-lineage selection

Paco Majic[1,*], Malvika Srivastava[2] & Justin Crocker[1]

[1]European Molecular Biology Laboratory, 69117 Heidelberg, Germany

[2]Department of Ecology and Evolution, University of Lausanne, 1015 Lausanne, Switzerland

*Paco Majic

Email: paco.majic@embl.de

Abstract

Mutation rates drive the pace and potential of evolutionary change. However, to better understand the evolutionary implications of mutation rates, there is a need to uncover the causes of their diversification. In multicellular organisms, all mutations first arise in a single cell in a developmental context. Whether a mutation enters a population's gene pool can therefore depend on developmental events that affect the likelihood of mutant cell lineages of producing gametes. For this reason, the evolution of mutation rates in populations is governed not only by changes in the rates at which mutations occur at the molecular level, but also by changes in developmental features of organisms and how mutations impact cellular fitness during development. We present a theoretical framework that, supported by empirical data from mammals and experiments on the fruit fly, demonstrate how generational mutation rates can be shaped by changes in developmental parameters and intraorganismal selective processes even when molecular mutation rates are presumed constant. Our model highlights how the diversity of mutation rates observed across animals may be the byproduct of organismal development rather than the result of direct selection against mutator alleles. As such, development not only introduces phenotypic biases, it also shapes the rates and trajectories of genetic diversity and is thus at the core of evolutionary theory.

Main Text

"Seen from this point of view, life appears as a current which goes from germ to germ through the intermediation of a developed organism"

- Henri Bergson, *Creative Evolution*

Introduction

How genetic variation arises within a population shapes evolutionary trajectories (1-8). The rates of mutations in a population may affect how promptly adaptive genotypes may be encountered, while also defining how deleterious mutations may burden populations. Thus, mutation rates are closely tied to the pace and potential of evolutionary change. Although classical models presumed substitution and mutation rates to be relatively constant across the tree of life (9, 10), advances in molecular biology have progressively challenged this view (11-14). The depth and granularity at which we can now explore genetic diversity suggest that mutation rates are an evolvable trait, varying not only between clades (15-17), but also within species (18) and populations (19), underscoring their dynamic role in shaping genetic diversity.

The diversification of mutation rates can be shaped by the evolution of mutator alleles, defined as "any genomically encoded modifier of the mutation rate" (20). These alleles are typically considered to operate at the molecular scale, altering the balance between DNA damage and repair through variations in genes involved in these processes (14, 17, 20-23). Mutator alleles that promote hypermutation may be favored under strong adaptive pressures (19, 24), while those causing excessive deleterious mutations would be selected against (25, 26). Because most mutations tend to be deleterious, the mutation rates of species are thought to be dominated by the efficacy of selection in purging alleles that increase the rates of mutations (26). This is why the drift-barrier hypothesis posits that the efficiency of selection against mutator alleles depends on population size. Larger populations can better counteract genetic drift, resulting in lower mutation rates, whereas smaller populations experience weaker selection against mutators and, thus, higher mutation rates (20, 26, 27). This view suggests that mutation rates evolve primarily through changes in molecular mechanisms constrained by selection. However, mutation rates

may also evolve through non-molecular causes. A relevant factor in this regard is generation time and age at reproduction, which influence the number of mutations germlines accumulate before reproduction (28-31).

Another non-molecular factor that may influence mutation rate evolution is that, in multicellular organisms, new mutations necessarily arise in a single cell in the organismal context of each parent. For a mutation to enter the population's gene pool, it must propagate within the organism and be part of the germline, meaning developmental traits have the potential to shape the likelihood of heritable mutations. For instance, the timing of germline determination (32), and differences in gamete production between sexes or species can influence mutation rates (16, 30, 31, 33). Moreover, mutations may result in differences in cellular fitness, which can greatly influence the genetic diversity existing within organisms. In the germline context, mutations that affect the fitness of cells relative to their sisters may bias their own heritability if they occur on the lineage of cells that go from zygote to gamete (34-41). Such bias can have important evolutionary repercussions (40): it may affect the probability of fixation of variants that alter cell fitness, it allows for a "cheap" purging of deleterious variants, and it can also promote evolvability when the impact of mutations on cellular fitness and on individual fitness align. Nevertheless, cell-lineage selection tends to be overlooked in discussions of mutation rate evolution (17, 22, 30), and it is generally unaccounted for in mutation rate estimations, since whenever selection is considered there is a tendency to focus exclusively at the level of individuals - a perspective which biases causal explanations of mutation rate variation (36).

In this work, we emphasize the view that differences in population-level mutation rates across species may result from causes other than molecular changes mediated by mutator alleles. Using analytical models, data analysis and experiments in *Drosophila,* our work consolidates a view of mutation rate evolution, which demonstrates how the interplay of developmental and life-history parameters with intraorganismal selection on mutant cells can majorly affect the rate of new mutations in a population. This perspective has important conceptual implications for understanding the evolution of mutation rates. Unlike explanations like the drift-barrier hypothesis, our model highlights how developmental processes may influence generational mutation rates, positioning them as a byproduct of organismal development rather than direct selection at the level of individuals in a population. Furthermore, this model broadens the role of

85 organismal development in population genetics: development not only introduces phenotypic
86 biases, but it also shapes the rates and trajectories of genetic diversity, which places development
87 at the core of evolutionary theory.

88 **Results**

89 A theoretical framework to assess the influence of developmental features and cell-lineage
90 selection on mutation rate diversification

91 To distinguish between the molecular mutation rate, μ_{mol}, and the mutation rate per generation
92 at the population level, μ_{pop}, we revisited the theoretical framework of Otto & Orive (35), who
93 explored how the mutation load of a population is affected by intraorganismal selection within
94 individuals (see Methods). Conceptually, development is modeled as a branching tree of cell
95 lineages, with μ_{pop} partly determined by the number of cells carrying a mutation at locus *i* at the
96 end of development, M_i (Figure 1A). M_i is a function of:

97 i) a molecular variable μ_{mol}, which is the mutation probability per cell per locus per unit of
98 developmental tempo, which can be either per cell division when mutations are of
99 replicative nature (35), or per time unit when they result from other sources of DNA
100 lesions (29, 42),
101 ii) developmental parameters such as the duration of development (τ), and the rate of cell
102 proliferation (C), and
103 iii) the effect of mutations at locus *i* on cell fitness (β_i), which alters the rate of cell
104 proliferation of mutant cells relative to nonmutant cells in the developmental context. β_i
105 < 1 indicates deleterious effects that decrease cell proliferation, β_i = 1 neutrality, and β_i
106 > 1 beneficial effects that increase proliferation.

107 With an estimation of M_i and assuming that germline determination is independent of mutational
108 events, it is then possible to calculate μ_{pop} at locus *i* as the probability of sampling a mutant cell
109 among the total pool of cells, which includes all M_i mutated cells as well as all cells that completed
110 development without mutations, N_i. Such that:

111 $$\mu_{pop_i} = \frac{M_i}{M_i + N_i}$$

112 By defining μ_{pop} as the probability of randomly sampling mutant cells at the end of development,
113 we are implying that this probability also encompasses the probability that sampled cells are of
114 the germline lineage that goes from the zygote to differentiated gametes. This captures aspects
115 of development such as how body size, which scales with the total number of cells, generally
116 reflects germline size (43). However, our model does not consider many nuances of actual
117 development. Development is highly structured with different cell lineages proliferating and
118 differentiating at different tempos. Furthermore, overproliferation of cells by means of increases
119 in β_i could result in tumorigenesis, which would affect μ_{pop} through deleterious effects on
120 individual fitness. However, more often than not, mutant alleles spread selectively within healthy
121 tissues without causing tumors or deleterious effects on organismal fitness (44-50). This is not
122 only true for somatic tissues, but also for the germline (41). Our formalization is therefore
123 sufficient to assess how fundamental developmental features in combination with cell-lineage
124 selection can influence the rates at which mutations enter a population's gene pool, regardless of
125 their effect on organismal fitness and even if the molecular mutation rate μ_{mol} is constant.

126 <u>Developmental parameters can influence the diversification of mutation rates</u>

127 As per our model, under neutral conditions (β_i = 1), evolutionary lineages that increase τ, also
128 increase the expected μ_{pop} for locus *i* (Fig. 1B). This is also the case for shifts in *C*, but only if μ_{mol}
129 is considered to track cell divisions (Fig. 1B). When considering μ_{mol} to track mutations per unit
130 time, μ_{pop} also increases as a function of τ, but it is only affected by changes in *C* only if changes
131 in the rate of cell proliferation also result in changes in τ (Fig. S1A). To evaluate whether these
132 developmental parameters may explain interspecific differences in μ_{pop}, we analyzed estimates of
133 μ_{pop} (16) for a number of amniote species. Focusing on the mammalian clade, which has the most
134 comprehensive phylogenetic sampling (Fig. 1C, Table S1) and developmental information (51), we
135 focused on gestation time as a proxy for τ, as well as on the body mass as a proxy for total cell
136 count, proportional to $2^{C\tau}$ (52). As predicted by our model, the μ_{pop} of mammals positively
137 correlated with the proxy τ (Fig. 1D, Pearson's $\rho = 0.49$, $p = 0.0025$), as well as $2^{C\tau}$ (Fig. S1B,
138 Pearson's $\rho = 0.48$, $p = 0.0029$).

139 To more directly address the question of whether developmental parameters could account for
140 the interspecific diversification of μ_{pop}, we compared these variables between sister clades in our
141 phylogeny by calculating the ratio of μ_{pop} and body mass (Methods). We found that the majority
142 of the comparisons between relatively recently diverged species (Fig 1C, black bars) yielded a
143 correlation such that the larger of both species tended to have higher μ_{pop} (Fig. 1E, black dots). In
144 79% of recently diverged species pairs the larger of both species also had a higher μ_{pop}, which was
145 significantly different from random pairs (Fig. S1C, p = 0.01, one-sample permutation test). For
146 example, the estimated μ_{pop} of domestic cats (*Felis catus*) is ~2 times lower than that of tigers
147 (*Panthera tigris*) and ~2.5 times lower than that of leopards (*Panthera pardus*), while the μ_{pop} of
148 walruses (*Odobenus rosmarus*) is ~1.95 times that of the much smaller Antarctic fur seals
149 (*Arctocephalus gazella*). Interestingly, this held not only for mammals but also for birds, even if
150 the phylogenetic granularity of estimated μ_{pop} is lower (Fig. S2, in 74% of comparisons of related
151 bird species pairs the larger of both species also had a higher μ_{pop}, p = 0.02, one-sample
152 permutation test). Therefore, as lineages diverge, we expect that if either lineage tends to
153 increase in size, its mutation rate will also tend to increase. We do note that body size is also
154 correlated with generation time, and that the correlation between generation time and μ_{pop} (16),
155 as well as the influence of parental age at reproduction (53), may bias our interpretation. But, if
156 developmental parameters affecting body mass or other correlated life history traits are indeed
157 affecting μ_{pop}, then the diversification of developmental parameters may offer a non-molecular
158 explanation for observed diversification patterns of mutation rates.

159 As mentioned above, according to the drift-barrier hypothesis, the negative correlation existing
160 between the generational mutation rates of species and their effective population sizes could be
161 due to the efficacy of selection against alleles affecting μ_{mol} (20, 26). However, that relationship
162 could also be the neutral byproduct of changes in developmental parameters affecting body size,
163 rather than the selective purging of mutator alleles. This is because mammals follow a global
164 scaling relationship between body size and population density described by Damuth's rule (54),
165 as well as with the effective population size (17). Considering that body mass is proportional to
166 the total number of cells in a body, then τ and C not only affect μ_{pop}, but also the demographic
167 properties of a population. Therefore, simply considering the predicted effective population size
168 for different values of $C\tau$ based on this proportionality produces an inverse relationship between

169 the mutation rate of a species and its effective population size (Fig. 1F), as would also be expected
170 from the drift-barrier hypothesis. Thus, the differences in mutation rates observed in populations
171 of different sizes may be the result of changes in developmental parameters that, because of
172 ecological and energetic reasons, may also relate to changes in population sizes (55).

173 <u>The embryonic selective environment and its effect on mutation rates</u>

174 So far, we have been considering the case in which mutations are selectively neutral at the cellular
175 level. In other words, we have been considering the case where $\beta_i = 1$. However, if we take into
176 account how mutations may impact their own heritability by affecting cellular fitness, a selective
177 regime in the embryo or body of an organism can then also affect μ_{pop} without changes in μ_{mol}
178 (Fig. 2A). Cellular fitness could be affected by various processes, including the migration of cells,
179 proliferation, and, in the specific case of germline cells, the determination and maintenance of
180 the germline cell fate. Mutations on genes involved in these processes may end up under- or over-
181 represented in the gamete pool produced by an organism (41, 56).

182 To explore how mutations affecting β_i as in our model may impact their own heritability, we
183 considered the *Drosophila melanogaster* gene *trithorax-related (trr)*, which influences cell
184 proliferation (57). We generated mutant clones by inducing mitotic recombination through the
185 FLP/FRT technique (58) on flies that carried both a sub-functional allele of *trr* (TrrCA,(59)) on an
186 unmarked chromosome and a wild-type version of the gene (TrrWT) on a chromosome marked
187 with a *red fluorescent protein, mRFP* (see Methods). As a result, within a single embryo, some cells
188 are homozygotic for TrrCA, homozygotic for TrrWT, or heterozygotic with a copy of each allele
189 (Fig. 2B). Because an impaired *trr* activity increases the rates of cell proliferation (57), we then
190 expected that $\beta_{trrCA/trrCA} > \beta_{trrWT/trrCA} > \beta_{trrWT/trrWT}$ and, therefore, that the TrrCA allele would be
191 overrepresented in the germline and thus have a higher heritability than TrrWT. Consistent with
192 this hypothesis, when mosaicism was induced early in development, a median of ~55% of
193 offspring carried the mutant allele, a fraction that was significantly higher than the cases when
194 mosaicism was not induced on the TrrCA/TrrWT heterozygotes or when it was induced in the lines
195 with two copies of TrrWT (Fig. 2C). This experiment illustrates how a mutation inducing a greater
196 proliferation of cells that carry it can increase its own heritability, representing a case of what
197 Otto and Hastings referred to as "mitotic drive" (40).

198 In our model, varying the proliferative effect β_i of a mutation on a cell can drastically change the
199 effective μ_{pop} even when molecular mutation rates are constant, such that higher values of β_i
200 imply higher μ_{pop} (Fig. 2D). A relevant insight from this model is that even mild consequences for
201 cellular proliferation may have major consequences for the rate at which new mutations enter
202 the gene pool of populations. For example, in the case of $C\tau = 20$ (representing 2^{20} cells, roughly
203 the number of ovarian follicles an infant is born with (60) or half of the number of germ cells in
204 the ovary of cows by the third trimester of pregnancy (61)), a mere 1% increase ($\beta_i = 1.01$) or
205 decrease ($\beta_i = 0.99$) in cell fitness may result in a ~7% change in μ_{pop} (Fig. 2D).

206 The effect of β_i on μ_{pop} also depends on the developmental parameters C and τ (Fig. 2D). Higher
207 values of $C\tau$ tend to produce larger differences in μ_{pop} for large β_i . On the other hand, when β_i is
208 small, $C\tau$ does not have a strong effect on the mutation rate. We note that when $\beta_i \neq 1$, changes
209 in C and τ, also affect μ_{pop} when μ_{mol} is considered as mutations per unit of time, rather than per
210 cell division (Fig. S3A). This contrasts with the aforementioned neutral case, where changes in C
211 did not change μ_{pop} for constant τ (Fig. S1A).

212 Our model, therefore, suggests that: i) the selective consequences of mutations at the cellular
213 level may influence generational mutation rates, and ii) the magnitude of this influence depends
214 on developmental parameters. Specifically, our model predicts that organisms of larger size and
215 slower development should be more efficient in purging mutations that are deleterious for cells
216 and more prone to facilitate the fixation of mutations that are beneficial to cells (Fig. 2D). This
217 shows how differences in mutation rates between species may be enhanced by developmental
218 differences, and it highlights how the relevance of cell-lineage selection as a “cheap" way to filter
219 deleterious mutations (40) may be evolve by shifting developmental parameters.

220 <u>The interplay between cellular distribution of fitness effects and developmental parameters</u>

221 The effect of mutations on cellular fitness is expected to vary across genes, depending on their
222 involvement on cellular processes, and even across loci within genes, depending on their
223 relevance for gene function. For example, in our *Drosophila* case study, despite carrying a
224 mutation in the gene *white* (*w*) (Methods), the TrrWT allele did not lead to differences in
225 heritability in our FLP/FRT experiments (Fig. 2C). This suggest that even though mutations on *trr*

226 can influence β_i, mutations on *w* do not, which implies that *trr* and *w* likely contribute differentially
227 to μ_{pop}.

228 To explore how differences in β_i at different loci affects genome-wide mutation rate estimations,
229 we adjusted our developmental model such that the overall genomic mutation rate would be
230 proportional to the fraction of sites that have either deleterious ($F_{\beta<1}$), neutral ($F_{\beta=1}$) or
231 advantageous ($F_{\beta>1}$) fitness effects on cells (Methods). Moving from a case in which mutations
232 on all sites are neutral for cellular fitness ($F_{\beta=1} = 1$,), to a case in which all mutations are strongly
233 deleterious ($F_{\beta=0} = 1$), there is a steady drop in the expected μ_{pop}, tending towards μ_{mol} as most
234 mutations become deleterious (Fig. 2E). Considering cases in which most mutations are either
235 neutral or deleterious for cellular fitness would be in accordance with what is expected (25). In
236 contrast, scenarios in which many mutations tend to increase cellular fitness are presumably rare.
237 However, our model does suggest that even if infrequent, mutations with strong beneficial effects
238 on the fitness of cells can drastically influence the genome-wide estimations of μ_{pop}. Depending
239 on the developmental parameters $C\tau$, this is true if mutations that increase cellular fitness are 1
240 in 1000 ($F_{\beta>1} = 0.001$), or even 1 in a million ($F_{\beta>1} = 1x10^{-6}$) (Fig.2F). Notably, variations in
241 the ratios of $F_{\beta=1}$, $F_{\beta>1}$ and $F_{\beta<1}$ also vary the relationship between μ_{pop} and developmental
242 parameters (Fig. 1E,F).

243 Furthermore, because β_i affects mutated cells by altering their proliferative capacity, the number
244 of genome-wide mutations capable of increasing or decreasing cellular fitness may depend on the
245 rate of cell proliferation of wild-type cells. In other words, $F_{\beta=1}$, $F_{\beta>1}$ and $F_{\beta<1}$ may depend on
246 baseline *C,* such that for greater *C* there should be a smaller number of mutations for which $\beta_i >$
247 1. Such would represent a case of diminishing returns epistasis, according to which the fitness
248 effect of a mutation is milder when it occurs on a fit genotype than when it occurs on an unfit
249 genotype (62-64). Epistatic effects of this kind could explain why there is a negative correlation
250 between our estimates of *C* for a subset of mammalian species (Methods) and μ_{pop} (Fig. S3B,
251 Pearson's $\rho = -0.38$, $p = 0.044$), since greater $F_{\beta>1}$ imply greater μ_{pop} (Fig. 2F). This would mean
252 that whenever species evolve a greater size through increases in *C*, the cellular distribution of
253 fitness effect could change as well, thus affecting μ_{pop}.

254 Therefore, the genome-wide distribution of cellular fitness effects of mutations interacts with and
255 may be defined by the developmental background of an organism to jointly influence μ_{pop}. A
256 factor that needs consideration in any interpretation of differences in mutation rates between
257 species using genomic data.

258 Selection in the mature germline stem cell niche

259 In addition to embryonic development, the lifetime of organisms could also shape μ_{pop}. This could
260 take place, as mentioned earlier, because longer generations imply a greater accumulation of new
261 mutations before reproduction (30, 65, 66). Here, we argue that this could also be because of the
262 dynamic competition between germline stem cells of different genotypes. During an individual's
263 lifetime, germline stem cell niches can undergo a cellular turnover. In mice, for example,
264 spermatogenic stem cells sometimes cease to be stem cells and are replaced by neighboring stem
265 cells, keeping the number of stem cells relatively constant (67). Although the repopulation of
266 these cleared niches by neighboring cells could be a stochastic process (68), mutations that affect
267 the rate of stemness loss (either through death or differentiation) might eventually create a
268 mosaic of spermatic stem cells with an overall higher fitness (41, 56). Thus, a selective cell
269 turnover might impact the repertoire of mutations that a single individual can introduce into a
270 population's gene pool.

271 To incorporate the effect of selection during the lifespan of an organism, we built on our
272 developmental model described above and included a maturation and reproductive phase (Fig.
273 3A, Methods). In this adapted version, at the end of development, there is a final and constant
274 pool of stem cells that can produce gametes, $M_{t=0}$ of which are mutated. These cells can undergo
275 a turnover, either because of a death-birth dynamic in the stem cell niche or because of
276 differentiation. This turnover of cells in the stem cell niche occurs at a rate *d* over an arbitrary unit
277 of time *t* subdividing the total generational time *l*, and a new selective variable β_m which describes
278 the fitness effect of mutation on cells related to stem cell turnover during the lifetime of an
279 organism. In this model, in the case when there is no turnover of cells during the lifetime of an
280 individual (d = 0) or when mutations are neutral ($\beta_m = 1$), μ_{pop} only changes due to the
281 mutational accumulation of new mutations. Whenever there is a turnover of cells and mutations
282 do affect the proliferative capacities of cells, a positive effect of mutations on the fitness of cells

283 increases the overall μ_{pop} while deleterious mutations decrease it closer to μ_{mol} (Fig. 3B). This
284 effect is more pronounced for individuals that take longer to reproduce (Fig. 3C).

285 The intraorganismal selective process over the lifespan of a mature organism may interplay with
286 the intraorganismal selective process taking place earlier during development to shape an
287 effective μ_{pop} (Fig. 3D). For example, mutations on genes involved in basic cellular functions
288 would likely have fitness consequences for cells at any stage of an individual's life, thus affecting
289 cell proliferation during development, but also the rates of germline stem cell turnover ($\beta > 1$, β_m
290 > 1). On the other hand, there may be genes that are irrelevant for cellular fitness in the germline
291 stem cell niche that may be important during development ($\beta \neq 1$, $\beta_m = 1$) and vice versa ($\beta = 1$,
292 $\beta_m \neq 1$). The latter would be the case of mutations on the *chimno* mutants in *Drosophila*, which
293 have been reported to evict wild-type cells from the stem cell niche of the testis (38). It is also
294 possible that the selective regime during development and maturity point in opposite directions,
295 which is what we observed in the case of the TrrCA mutation presented above: even though
296 mosaic females introduced in Fig. 2C produced a progeny that was biased in favor of the *trr*
297 mutant allele right after pupation, as those same females aged, the biased shifted in favor of
298 TrrWT (Fig. 3E), suggesting that for this allele $\beta > 1$ and $\beta_m < 1$. On the other hand, as expected,
299 TrrWT retained a $\beta = \beta_m = 1$ through the development and lifespan of each female fly (Fig. 3F).

300 These results reinforce the notion that the estimation of global genome-wide mutation rates may
301 lead to biased interpretations of the molecular rates because of the fitness consequences of
302 mutations on different loci. More generally, our results also support that the overall expected
303 μ_{pop} is likely the composite outcome of the selective effect of mutations at the cellular level
304 during development and maturity, as well as the life history traits of the organism.

305 **Discussion**

306 Mutations arise in organismal contexts that vary across individuals and species. As our results
307 demonstrate, these contexts significantly influence how genetic variation is produced and
308 incorporated into gene pools. Therefore, differences in population-level mutation rates may not
309 solely result from changes in molecular mutation rates or changes in generation time, but could
310 arise from evolutionary shifts in developmental parameters. These include the rate of cell

311 proliferation, developmental duration, germline differentiation modes, germline dynamics during
312 maturity, and—crucially—selective dynamics at the cellular level.

313 This perspective implies that it is not essential to invoke direct selection on mutation rates to
314 account for the observed diversity of mutation rates across multicellular lineages. This is not to
315 say that selection at the level of individuals plays no role in modulating mutation rates. Molecular
316 rates might indeed evolve, for example, to mitigate the burden of deleterious mutations,
317 particularly somatic mutations that can cause cancer in the case of larger and longer-lived species
318 (65, 69-71). However, because developmental parameters alone can produce substantial shifts in
319 mutation rates, as species evolve different morphologies and life history strategies, their rates of
320 genetic diversification can also diverge as a secondary outcome that may or may not be neutral.

321 Our results illustrate how the diversification of mutation rates can arise as a consequence of
322 changes in developmental parameters associated with body size evolution. This is supported both
323 by our theoretical model and by a general pattern in which the larger of two closely related
324 species tends to exhibit a higher generational mutation rate. However, this trend is not universal
325 and can be influenced- or even reversed- by other factors. Although body size typically correlates
326 with germline size (43), deviations from this relationship, such as disproportionate germline cell
327 numbers or developmental heterochronies in the gonads, can alter expected generational
328 mutation rates, as suggested to explain higher rates in chimpanzees relative to humans (72).
329 Additionally, developmental changes tied to body size may interact in complex ways with
330 intraorganismal selection. For instance, in the leopard-tiger and goat-dwarf musk deer species
331 pairs (Fig. 1C), the larger species shows a lower estimated generational mutation rate (red
332 arrowheads in Fig. 1E, Table S1). We speculate that this misalignment reflects a smaller fraction
333 of mutations capable of further increasing cellular proliferation ($F_{\beta>1}$) in species with an
334 inherently higher proliferative capacity of wild-type cells. We infer tigers and goats to have a
335 higher rate of cell proliferation per unit time (greater *C*) than leopards and dwarf musk deer,
336 respectively. This is evidenced by the fact that tigers, despite reaching larger birth sizes than
337 leopards, have similar developmental times, while dwarf musk deer, though significantly smaller
338 than goats, possess markedly longer developmental times (Table S1).

339 <u>The biological causes of mutation rate diversification</u>

340 The diversification of developmental parameters not only provides a basis for hypotheses about
341 species-specific shifts in shifts in mutation rates, but also offers potential explanations for well-
342 established patterns of mutation rate diversification. Our results suggest that the prevalent
343 negative correlation between generational mutation rates and population size (16, 17, 20, 26), is
344 more parsimoniously explained by developmental variations accompanying lineage divergence
345 than by recurrent selective adjustments of molecular mutation rates in response to demographic
346 changes, as proposed by the drift barrier hypothesis (26). Given that ecological drivers may
347 influence body size evolution (55) and that developmental parameters that increase body size
348 also increase generational mutation rates, the co-adjustment of population size and
349 developmental properties (or correlated life history traits) could underlie the diversification of
350 generational mutation rates. Although the drift barrier hypothesis is supported by various studies
351 that show a correlation between mutation rates and effective population size across clades (17),
352 we are here suggesting that, at least for multicellular organisms, there are other biological
353 properties that may explain the same trend, or at least reinforce it. This is consistent with our
354 findings and supported by evidence that diversification in mutation spectra, often attributed to
355 molecular changes, primarily occurs between distantly related lineages (73) and may also be
356 influenced by environmental factors (74) or cell cycle dynamics (23).

357 The developmental influence on generational mutation rates also offers alternative explanations
358 to other patterns of mutation rate variability that have been attributed to changes in molecular
359 mutation rates. An example is the differential accumulation of mutations during different stages
360 of mouse development, which has been interpreted to be the result of a stage-specificity of DNA
361 repair systems (75), but that could be explained by a stage-specificity of any of the developmental
362 parameters we explored. Another example is the negative correlation between the generation
363 times of species and their estimated yearly mutation rates (76). A proposed explanation aligning
364 with the drift barrier hypothesis is that gamete mutation rate modifiers are constrained by the
365 product of population size and generation time by selection at the individual level (65). Our intra-
366 organismal selection model predicts similar trends, albeit through a different mechanism: longer-
367 lived species allow more efficient elimination of variants that are deleterious the cellular level and
368 a greater retention of beneficial ones due to extended selective dynamics. Thus, if most mutations
369 tend to negatively affect cellular fitness, which, as discussed above, may be the case for larger

370 organisms that also have longer generation times, intraorganismal selection would produce lower
371 estimations of yearly mutation rates for species with longer generation times.

372 Developmental parameters and intraorganismal selection shape not only interspecific differences
373 in mutation rates, but may also help explain variation within species. A well-established pattern
374 is the higher mutation rates in males compared to females in the germlines of mammals and birds,
375 a bias largely absent in reptiles and fish, where reproductive biology is more similar between sexes
376 (16). The male-bias in birds and mammals has been attributed to a greater cell division number
377 during the lifetime of males (30), but also to imbalances in the DNA repair mechanisms between
378 the sexes (77). But sex-specific biases could also be caused by intraorganismal selection (40, 41,
379 56). The selective expansions of mutant lineages in the male germline may exacerbate the
380 differences in generational mutation rates, including the paternal age effect (78), as has been
381 reported from clinical cases (41, 79, 80). In terms of our model, male-specific expansions are
382 facilitated by a greater stem cell turnover over the lifetime of organisms, with females having $d \sim$
383 0 and males $d > 0$ (Fig. 3B). Interestingly, if intraorganismal selection is at least partially driving
384 the differences between male and female mutation rates, we expect not only a quantitative bias,
385 but also a qualitative bias: whereas mutations inherited from females would be enriched in
386 mutations that are deleterious to cells and would likely get purged if that mutation arose in the
387 male germline, mutations inherited from fathers are likely enriched in effects increasing cell
388 fitness.

389 Although our argument broadly aligns with the idea that non-molecular causes may underlie the
390 diversification of generational mutation rates (28, 29, 33), we do not rule out the evolutionary
391 relevance of molecular mechanisms. Alterations to baseline molecular mutation rates are well-
392 documented (81) and likely coexist with intra-organismal selection and developmental influences
393 (36, 82). Disentangling whether a particular molecular, developmental or life history parameter
394 has driven the diversification of generational mutation rates between species may be challenging,
395 as many relevant factors tend to be correlated. But ultimately, the causes of mutation rate
396 diversification are likely multifaceted. In this context, we propose an expansion of the definition
397 of "mutator alleles" (20) beyond molecular mechanisms that affect DNA repair and damage.
398 Instead, mutator alleles may also expand to genes that influence developmental processes, life
399 history traits, or organismal physiology.

400 Considerations about the place of development in evolution

401 The role of development in evolution is increasingly recognized, but much of the discussion has
402 focused on how developmental systems constrain or drive phenotypic evolution (83-86). Our
403 findings emphasize an additional role: by influencing mutation rates, development can shape the
404 evolutionary pace and direction at both phenotypic and genotypic scales.

405 In the conceptual framework of genotype space (87), populations could, in principle, explore the
406 space equally in all directions (Fig. 4A). However, mutational biases—such as the well-
407 documented transition versus transversion bias—skew this exploration (Fig. 4B), affecting the
408 spectrum of adaptive substitutions available to populations (4). Beyond molecular biases,
409 developmental processes can further constrain or promote specific directions of exploration (Fig.
410 4C) and influence the breadth of genotype space sampled within a generation (Fig. 4D). This has
411 quantitative and qualitative implications for the genetic diversity of populations. Quantitively,
412 populations of larger organisms like rheas, for example, can explore a broader portion of genotype
413 space compared to those of smaller organisms like gulls, which have a considerably smaller
414 generational mutation rate (16). While qualitatively, this broader exploration may occasionally
415 introduce deleterious variants, many of these—particularly those disrupting basic cellular
416 functions or germline potential—are more efficiently pruned in larger species due to their
417 developmental and intraorganismal selective dynamics. Thus, organisms are not merely vehicles
418 for genes, as major evolutionary paradigms suggest (88). Instead, development actively
419 participates in shaping genotypic changes arising in the gene pools of populations and, by
420 extension, the evolutionary trajectories of species.

421 Overall, by highlighting the interplay between development and selection at the cellular level, we
422 provide a broader framework for understanding the diversification of mutation rates. Taking this
423 framework into account, we suggest that future studies exploring the diversification of mutation
424 rates should account for the developmental contexts in which mutations arise in each species and
425 the ecological interactions between cells of different genotypes.

426 **Materials and Methods**

427 Developmental model for estimation of μ_{pop}

428 We define the generational mutation rate μ_{pop} as the probability of sampling a mutant cell among
429 all cells in an organism that are capable of producing gametes at the time of reproduction of an
430 individual. To calculate this probability, it is necessary to first calculate M_i, which represents the
431 total number of cells that are expected to carry a mutation at a given locus *i*. We adapted a model
432 from Otto & Orive (35), wherein M_i is a function of the molecular mutation rate μ_{mol}, the total
433 developmental time τ, the rate of cell divisions during development C, and a factor β_i, which
434 represents the effect of a mutation on the fitness of a cell carrying a mutation on locus *i*. At
435 developmental time *x*, one would expect $2^x(1-\mu_{mol})^{x-1}$ cells to not carry any mutations. Each
436 of those cells can mutate with a probability given by μ_{mol} and the mutated lineage will then
437 undergo $\beta_i(C\tau - x)$ cell divisions more until the conclusion of development. Thus, the number of
438 mutant cells resulting from mutations at time *x* is:

439 $$2^x(1-\mu_{mol})^{x-1} * \mu_{mol} * 2^{\beta_i(C\tau - x)}$$

440 Summing over all *x* gives us M_i at the conclusion of development:

441 $$M_i = \sum_{x=1}^{C\tau} 2^x(1-\mu_{mol})^{x-1} * \mu_{mol} * 2^{\beta_i(C\tau - x)}$$

442 For estimating μ_{pop} it is also necessary to calculate the expected number of cells that do not
443 undergo mutations at locus *i* through the course of development i.e., N_i. This can be calculated
444 as:

445 $$N_i = 2^{C\tau}(1-\mu_{mol})^{C\tau}$$

446 The total number of cells at the end of development is $(M_i + N_i)$ and thus μ_{pop_i} approximates the
447 probability of sampling a cell mutated at locus *i* from all cells in the pool of gametes, such that

448 $$\mu_{pop_i} = \frac{M_i}{M_i + N_i}$$

449 The calculations shown above correspond to those considering μ_{mol} to track cell divisions. In the
450 cases in which mutation rates are taken to track time rather than cell divisions, the calculations
451 for M_i and N_i were modified such that,

452 $$M_i = \sum_{x=1}^{\tau} 2^{Cx}(1-\mu_{mol})^{x-1} * \mu_{mol} * 2^{\beta_i C(\tau - x)}$$

453 And,

454 $$N_i = 2^{C\tau}(1-\mu_{mol})^{\tau}$$

455 To estimate μ_{pop} across the entire length of a genome, as a first order approximation, we assumed
456 that no cell obtains mutations at more than one locus during the entire course of development.
457 In other words, we assume ${\mu_{mol}}^2 \approx 0$. This assumption would hold for very small μ_{mol}. Using this
458 simplification, we can estimate μ_{pop} across the entire length of a genome by averaging μ_{pop} across
459 all sites with different values of β_i. In our model, we considered $F_{\beta i=f}$ to be the fraction of the
460 total sites in a genome that have a $\beta_{i=} f$, giving:

461

462 $$\mu_{pop} = \sum_{f} \mu_{pop_i}(\beta_i = f) \cdot F_{\beta i=f}$$

463 <u>Expansion of the model to account for maturation and time to reproduction</u>

464 To consider the role of lifetime of an organism in the calculation of $\mu_{pop,}$ we considered the pool
465 of cells resulting from the developmental process to be constant in number. Immediately at the
466 end of development, there are $M_{t=0}$ cells in the germline stem cell niche that are mutated and $N_{t=0}$
467 that are not. During an organism lifetime *l,* germline stem cells can undergo a turnover (due to
468 differentiation or death) at a rate *d* over an arbitrary unit of time *t*. The rate at which mutant cells
469 replace lost cells during this turnover is given by a selective variable β_m. As in the case of the
470 developmental selective parameter β, when $\beta_m < 1$ mutations are deleterious, when $\beta_m = 1$
471 mutations are neutral and when $\beta_m > 1$ mutations are advantageous to cells. In our model,

472 during the lifetime of an organism before reproduction, it is possible for the total pool of mutated
473 cells to decrease either due to reverse mutations (which would occur at a low rate, $M_{t-1}\mu_{mol}$) or
474 loss due to death or differentiation (dM_{t-1}). Furthermore, mutant cells can increase in proportion
475 whenever non-mutant cells in the stem cell niche mutate ($N_{t-1}\mu_{mol}$) or whenever mutant cells
476 proliferate to replenish the stem cell niche after the loss of sibling cells. The number of mutated
477 cells at time *t* during the lifetime of an organism can thus be calculated as,

478 $$M_t = M_{t-1} + N_{t-1}\mu_{mol} - dM_{t-1} - M_{t-1}\mu_{mol} + \frac{\beta_m d(M_{t-1} + N_{t-1})M_{t-1}}{\beta_m M_{t-1} + N_{t-1}}$$

479 And the number of non-mutant cells would be given by

480 $$N_t = N_{t-1} + M_{t-1}\mu_{mol} - dN_{t-1} - N_{t-1}\mu_{mol} + \frac{d(M_{t-1} + N_{t-1})N_{t-1}}{\beta_m M_{t-1} + N_{t-1}}$$

481 <u>Comparison of μ_{pop} for different mammalian species</u>

482 To corroborate the predictions of our model we considered estimations of the μ_{pop} of each of 36
483 species of mammals. We considered the μ_{pop} of each species to be the mean of the number of de
484 novo mutations per base pair across different numbers of parent-offspring trios (16). We collected
485 the other biological parameters used, namely the body mass of each species and the gestation
486 time, from the Encyclopedia of Life (51). The phylogenetic relationships we considered were
487 based on recent phylogenetic assessments of mammals (89), while the estimated divergence
488 times were collected from various sources listed in Table S1. To estimate *C*, we considered
489 gestation times as a proxy for τ and the mass of neonates as a proxy for $2^{C\tau}$ for those species for
490 which this information was available in the Encyclopedia of Life.

491 To consider how the mutation rates of recently diverged species have evolved in relation to
492 developmental parameters, we compared the ratios of the body mass for pairs of species with
493 the ratios of mutations rates measured by Bergeron et al (16). The pairs we used for our
494 comparisons consisted of pairs of the two most closely related species (Fig. 1C). In cases like those
495 of *Sus scrofa* that have more than one species that are equally closely related, we considered all
496 possible species pairs (Fig. 1C, black bars). For these comparisons, we considered the ratio of the

497 mutation rate or body size of the smaller of both species against that of the larger one. Thus, the
498 ratio of body sizes should be greater than 1 for all comparisons. If the ratio of mutation rates is
499 also greater than one, body size and mutation rates are aligned, while if it is smaller than one, the
500 smaller species have a greater mutation rate. To test the significance of our result, we compared
501 the alignment of the μ_{pop} and body size ratios (the percentage of comparisons for which μ_{pop}
502 ratios were greater than 1) with the expectation from 1000 random permutations of μ_{pop}. Pairs
503 of species were considered to be recently diverged if their common ancestor dates back to less
504 than 65 mya (black bars in Fig. 1C, older pairs are not shown in the phylogeny but we used them
505 for our comparisons, Fig. 1E, gray point). The same analysis was carried out for the birds species
506 for which mutation rates were available (16), but no phylogenetic aging was assigned since all
507 extant birds diverged after the Cretaceous-Tertiary boundary of 65 my.

508 Estimation of effective population size (N_e) and the relationship between μ_{pop} and N_e

509 Organisms comprising of $2^{C\tau}$ cells, have a mass $m = m_{cell}\, 2^{C\,\tau}$, where $m_{cell} = 10^{-15} g$ is the
510 mass of a single cell (90). We used this mass estimate to compute the effective population size
511 N_e. This was done by using the scaling of effective population size and organism size (adult dry
512 weight) that was reported by Lynch et al. (17) for organisms across the tree of life. The fitted log–
513 log regression for the data resulted in the line: $\mathrm{y} = 6.717 - 0.199\mathrm{x}$. The above mass estimate
514 was also used to calculate the mutation rate μ_{pop} using our equation. Finally, we also compared
515 our predicted curve with mammalian weight and mutation rate data (see section above). Setting
516 μ_{mol} to $10^{-9.74}$ gave the best agreement with the empirical data.

517 Flippase assay to assess cell competition in fly germlines

518 We developed heat shock-induced mitotic clones in fruit flies following a standard protocol (58).
519 Briefly, a fly line (# 31418 from the Bloomington Drosophila Stock Center) containing a red
520 fluorescent protein (mRFP), a flippase-encoding gene induced by a heat-shock promoter (hsFLP)
521 and a FRT site for the binding of flippases was crossed with another line carrying a single-amino
522 acid substitution in the *trithorax-related* gene (*trr*) and the w^{1118} allele for the gene white. We thus
523 created a trr^{CA},w^{1118},FRT,hsFLP and a w^{1118},FRT,hsFLP lines. For our experiments we crossed these

524 lines with the parental mRFP,FRT,hsFLP lines and we exposed the heterozygotic embryos
525 collected during a window of four hours to a heat shock of 37°C for one hour.

526 We collected mosaic virgin females that developed from these heat-shocked embryos as well as
527 virgin females from embryos that were not heat-shocked (control). Each of these virgins were
528 individually paired to two w^{1118} males and we then counted the fraction of offspring that were
529 positive for red fluorescence, which are the ones that inherited the mRFP+ allele and not the
530 mRFP- (trr^{CA},w^{1118}) allele. For the same set of pairs, we evaluated the fraction of mRFP+ pupae
531 from offspring produced during the first week immediately after mothers were collected, as well
532 as during the second and third weeks.

533 **Acknowledgments**
534
535 We are grateful to Lautaro Gandara, Anna-Lena Vigil, David Porubsky and Cecilia Padilla Iglesias for their
536 useful feedback on our manuscript.
537
538 **References**

539 1. G. G. Simpson, *The major features of evolution*, Columbia biological series,
540 (Columbia University Press, New York,, 1953), pp. xx, 434 p.
541 2. L. Y. Yampolsky, A. Stoltzfus, Bias in the introduction of variation as an orienting
542 factor in evolution. *Evolution and Development* **3**, 73-83 (2001).
543 3. A. Stoltzfus, L. Y. Yampolsky, Climbing Mount Probable: Mutation as a Cause of
544 Nonrandomness in Evolution. *J Hered* **100**, 637-647 (2009).
545 4. A. V. Cano, H. Rozhoňová, A. Stoltzfus, D. M. McCandlish, J. L. Payne, Mutation
546 bias shapes the spectrum of adaptive substitutions. *Proc Natl Acad Sci U S A* **119**
547 (2022).
548 5. A. V. Cano, J. L. Payne, Mutation bias interacts with composition bias to influence
549 adaptive evolution. *Plos Comput Biol* **16** (2020).
550 6. M. Nei, *Mutation-driven evolution* (Oxford University Press, Oxford, ed. 1st,
551 2013), pp. xi, 244 p.
552 7. N. S. Martin, S. Schaper, C. Q. Camargo, A. A. Louis, Y. Kim, Non-Poissonian
553 Bursts in the Arrival of Phenotypic Variation Can Strongly Affect the Dynamics of
554 Adaptation. *Mol Biol Evol* **41** (2024).
555 8. D. Agashe, M. Sane, S. Singhal, Revisiting the Role of Genetic Variation in
556 Adaptation. *The American Naturalist* **202**, 486-502 (2023).
557 9. M. Kimura, The Rate of Molecular Evolution Considered from the Standpoint of
558 Population Genetics. *Proc Natl Acad Sci U S A* **63**, 1181-1188 (1969).
559 10. E. Zuckerkand, L. Pauling, Molecules as documents of evolutionary history. *J*
560 *Theor Biol* **8**, 357-366 (1965).

561 11. M. Kimura, Molecular evolutionary clock and the neutral theory. *J Mol Evol* **26**,
562 24-33 (1987).
563 12. T. H. Jukes, R. Holmquist, Evolutionary Clock: Nonconstancy of Rate in Different
564 Species. *Science* **177**, 530-532 (1972).
565 13. J. H. Gillespie, *The causes of molecular evolution*, Oxford series in ecology and
566 evolution (Oxford University Press, New York, 1991), pp. xiv, 336 p.
567 14. R. J. Britten, Rates of DNA Sequence Evolution Differ Between Taxonomic
568 Groups. *Science* **231**, 1393-1398 (1986).
569 15. Y. Wang, D. J. Obbard, Experimental estimates of germline mutation rate in
570 eukaryotes: a phylogenetic meta-analysis. *Evolution Letters* **7**, 216-226 (2023).
571 16. L. A. Bergeron *et al.*, Evolution of the germline mutation rate across vertebrates.
572 *Nature* **615**, 285-291 (2023).
573 17. M. Lynch *et al.*, The divergence of mutation rates and spectra across the Tree of
574 Life. *Embo Rep* **24** (2023).
575 18. K. Harris, Evidence for recent, population-specific evolution of the human
576 mutation rate. *Proc Natl Acad Sci U S A* **112**, 3439-3444 (2015).
577 19. P. D. Sniegowski, P. J. Gerrish, R. E. Lenski, Evolution of high mutation rates in
578 experimental populations of E. coli. *Nature* **387**, 703-705 (1997).
579 20. M. Lynch *et al.*, Genetic drift, selection and the evolution of the mutation rate.
580 *Nat Rev Genet* **17**, 704-714 (2016).
581 21. P. D. Sniegowski, P. J. Gerrish, T. Johnson, A. Shaver, The evolution of mutation
582 rates: separating causes from consequences. *Bioessays* **22**, 1057-1066 (2000).
583 22. A. C. Beichman, L. Zhu, K. Harris, The Evolutionary Interplay of Somatic and
584 Germline Mutation Rates. *Annual Review of Biomedical Data Science* **7**, 83-105
585 (2024).
586 23. N. Spisak, M. de Manuel, W. Milligan, G. Sella, M. Przeworski, The clock-like
587 accumulation of germline and somatic mutations can arise from the interplay of
588 DNA damage and repair. *PLOS Biology* **22** (2024).
589 24. F. Taddei *et al.*, Role of mutator alleles in adaptive evolution. *Nature* **387**, 700-
590 702 (1997).
591 25. M. Kimura, On the evolutionary adjustment of spontaneous mutation rates.
592 *Genetical Research* **9**, 23-34 (1967).
593 26. M. Lynch, Evolution of the mutation rate. *Trends in Genetics* **26**, 345-352 (2010).
594 27. W. Sung, M. S. Ackerman, S. F. Miller, T. G. Doak, M. Lynch, Drift-barrier
595 hypothesis and mutation-rate evolution. *Proc Natl Acad Sci U S A* **109**, 18488-
596 18492 (2012).
597 28. G. W. C. Thomas *et al.*, Reproductive Longevity Predicts Mutation Rates in
598 Primates. *Current Biology* **28**, 3193-3197.e3195 (2018).
599 29. Z. Gao, M. J. Wyman, G. Sella, M. Przeworski, Interpreting the Dependence of
600 Mutation Rates on Age and Time. *PLOS Biology* **14** (2016).
601 30. C. F. Baer, M. M. Miyamoto, D. R. Denver, Mutation rate variation in multicellular
602 eukaryotes: causes and consequences. *Nat Rev Genet* **8**, 619-631 (2007).

603 31. G. Amster, G. Sella, Life history effects on the molecular clock of autosomes and
604 sex chromosomes. *Proc Natl Acad Sci U S A* **113**, 1588-1593 (2016).
605 32. L. W. Buss, Evolution, development, and the units of selection. *Proc Natl Acad Sci*
606 *U S A* **80**, 1387-1391 (1983).
607 33. P. Moorjani, Z. Gao, M. Przeworski, Human Germline Mutation and the Erratic
608 Evolutionary Clock. *PLOS Biology* **14** (2016).
609 34. I. M. Hastings, Potential Germline Competition in Animals and Its Evolutionary
610 Implications. *Genetics* **123**, 191-197 (1989).
611 35. S. P. Otto, M. E. Orive, Evolutionary Consequences of Mutation and Selection
612 within an Individual. *Genetics* **141**, 1173-1187 (1995).
613 36. P. Majic, J. L. Payne, Developmental selection and the perception of mutation
614 bias. *Mol Biol Evol* 10.1093/molbev/msad179 (2023).
615 37. C. Extavour, A. García-Bellido, Germ cell selection in genetic mosaics in
616 Drosophila melanogaster. *P Natl Acad Sci USA* **98**, 11341-11346 (2001).
617 38. C.-Y. Tseng *et al.*, chinmo-mutant spermatogonial stem cells cause mitotic drive
618 by evicting non-mutant neighbors from the niche. *Dev Cell* **57**, 80-94.e87 (2022).
619 39. D. Haig, Mutational selection: fragile sites, replicative stress, and genome
620 evolution. *Qeios* 10.32388/9eryw5 (2023).
621 40. S. P. Otto, I. M. Hastings, Mutation and selection within the individual. *Genetica*
622 **102-3**, 507-524 (1998).
623 41. N. Arnheim, P. Calabrese, Germline Stem Cell Competition, Mutation Hot Spots,
624 Genetic Disorders, and Older Fathers. *Annual Review of Genomics and Human*
625 *Genetics* **17**, 219-243 (2016).
626 42. F. L. Wu *et al.*, A comparison of humans and baboons suggests germline
627 mutation rates do not track cell divisions. *PLOS Biology* **18** (2020).
628 43. G. J. Kenagy, S. C. Trombulak, Size and Function of Mammalian Testes in Relation
629 to Body Size. *Journal of Mammalogy* **67**, 1-22 (1986).
630 44. B. Colom *et al.*, Spatial competition shapes the dynamic mutational landscape of
631 normal esophageal epithelium. *Nature Genetics* **52**, 604-614 (2020).
632 45. A. R. J. Lawson *et al.*, Extensive heterogeneity in somatic mutation and selection
633 in the human bladder. *Science* **370**, 75-+ (2020).
634 46. I. Martincorena, P. J. Campbell, Somatic mutation in cancer and normal cells.
635 *Science* **349**, 1483-1489 (2015).
636 47. I. Martincorena *et al.*, Somatic mutant clones colonize the human esophagus
637 with age. *Science* **362**, 911-+ (2018).
638 48. I. Martincorena, P. H. Jones, P. J. Campbell, Constrained positive selection on
639 cancer mutations in normal skin. *P Natl Acad Sci USA* **113**, E1128-E1129 (2016).
640 49. I. Martincorena *et al.*, Universal Patterns of Selection in Cancer and Somatic
641 Tissues. *Cell* **171**, 1029-1041.e1021 (2017).
642 50. I. Martincorena *et al.*, High burden and pervasive positive selection of somatic
643 mutations in normal human skin. *Science* **348**, 880-886 (2015).

644 51. C. S. Parr *et al.*, The Encyclopedia of Life v2: Providing Global Access to
645 Knowledge About Life on Earth. *Biodiversity Data Journal* **2** (2014).
646 52. P. Alberch, S. J. Gould, G. F. Oster, D. B. Wake, Size and shape in ontogeny and
647 phylogeny. *Paleobiology* **5**, 296-317 (1979).
648 53. D. Porubsky *et al.*, Human de novo mutation rates from a four-generation
649 pedigree reference. *Nature* 10.1038/s41586-025-08922-2 (2025).
650 54. J. Damuth, Population density and body size in mammals. *Nature* **290**, 699-700
651 (1981).
652 55. J. D. Yeakel, C. P. Kempes, S. Redner, Dynamics of starvation and recovery
653 predict extinction risk and both Damuth's law and Cope's rule. *Nat Commun* **9**
654 (2018).
655 56. R. A. Hodge, E. A. Bach, Mechanisms of Germline Stem Cell Competition across
656 Species. *Life* **14** (2024).
657 57. H. Kanda, A. Nguyen, L. Chen, H. Okano, I. K. Hariharan, The Drosophila Ortholog
658 of MLL3 and MLL4, trithorax related, Functions as a Negative Regulator of Tissue
659 Growth. *Mol Cell Biol* **33**, 1702-1710 (2023).
660 58. K. G. Golic, S. Lindquist, The FLP recombinase of yeast catalyzes site-specific
661 recombination in the drosophila genome. *Cell* **59**, 499-509 (1989).
662 59. L. Gandara *et al.*, Developmental phenomics suggests that H3K4
663 monomethylation confers multi-level phenotypic robustness. *Cell Reports* **41**
664 (2022).
665 60. E. R. te Velde, P. L. Pearson, The variability of female reproductive ageing.
666 *Human Reproduction Update* **8**, 141-154 (2002).
667 61. K. C. Silva-Santos *et al.*, Estimate of the population of preantral follicles in the
668 ovaries of Bos taurus indicus and Bos taurus taurus cattle. *Theriogenology* **76**,
669 1051-1057 (2011).
670 62. B. Griffing, Analysis of Quantitative Gene Action by Constant Parent Regression
671 and Related Techniques. *Genetics* **35**, 303-321 (1950).
672 63. D. Aggeli, Y. Li, G. Sherlock, Changes in the distribution of fitness effects and
673 adaptive mutational spectra following a single first step towards adaptation. *Nat*
674 *Commun* **12** (2021).
675 64. E. R. Jerison, M. M. Desai, Genomic investigations of evolutionary dynamics and
676 epistasis in microbial evolution experiments. *Curr Opin Genet Dev* **35**, 33-39
677 (2015).
678 65. L. Zhu, A. Beichman, K. Harris, 10.1101/2023.12.06.570457 (2024).
679 66. E. Witt, C. B. Langer, N. Svetec, L. Zhao, Transcriptional and mutational
680 signatures of the Drosophila ageing germline. *Nat Ecol Evol* **7**, 440-449 (2023).
681 67. T. Nakagawa, Y.-i. Nabeshima, S. Yoshida, Functional Identification of the Actual
682 and Potential Stem Cell Compartments in Mouse Spermatogenesis. *Dev Cell* **12**,
683 195-206 (2007).

684 68. A. M. Klein, T. Nakagawa, R. Ichikawa, S. Yoshida, B. D. Simons, Mouse Germ Line
685 Stem Cells Undergo Rapid and Stochastic Turnover. *Cell Stem Cell* **7**, 214-224
686 (2010).
687 69. M. Lynch, The Cellular, Developmental and Population-Genetic Determinants of
688 Mutation-Rate Evolution. *Genetics* **180**, 933-943 (2008).
689 70. A. Cagan *et al.*, Somatic mutation rates scale with lifespan across mammals.
690 *Nature* **604**, 517-524 (2022).
691 71. G. W. C. Thomas, M. W. Hahn, The Human Mutation Rate Is Increasing, Even As It
692 Slows. *Mol Biol Evol* **31**, 253-257 (2014).
693 72. A. Wong, Covariance between Testes Size and Substitution Rates in Primates.
694 *Mol Biol Evol* **31**, 1432-1436 (2014).
695 73. A. C. Beichman *et al.*, Evolution of the Mutation Spectrum Across a Mammalian
696 Phylogeny. *Mol Biol Evol* **40** (2023).
697 74. L. B. Alexandrov *et al.*, Mutational signatures associated with tobacco smoking in
698 human cancer. *Science* **354**, 618-622 (2016).
699 75. S. J. Lindsay, R. Rahbari, J. Kaplanis, T. Keane, M. E. Hurles, Similarities and
700 differences in patterns of germline mutation between mice and humans. *Nat*
701 *Commun* **10** (2019).
702 76. L. Lewin, A. Eyre-Walker, K. Harris, Estimates of the Mutation Rate per Year Can
703 Explain Why the Molecular Clock Depends on Generation Time. *Mol Biol Evol* **42**
704 (2025).
705 77. F. L. Wu, M. de Manuel, M. Przeworski, A paternal bias in germline mutation is
706 widespread in amniotes and can arise independently of cell division numbers.
707 *eLife* **11** (2022).
708 78. J. M. Goldmann, J. A. Veltman, C. Gilissen, De Novo Mutations Reflect
709 Development and Aging of the Human Germline. *Trends in Genetics* **35**, 828-839
710 (2019).
711 79. S.-R. Yoon *et al.*, Age-Dependent Germline Mosaicism of the Most Common
712 Noonan Syndrome Mutation Shows the Signature of Germline Selection. *The*
713 *American Journal of Human Genetics* **92**, 917-926 (2013).
714 80. S.-K. Choi, S.-R. Yoon, P. Calabrese, N. Arnheim, A germ-line-selective advantage
715 rather than an increased mutation rate can explain some unexpectedly common
716 human disease mutations. *Proc Natl Acad Sci U S A* **105**, 10143-10148 (2008).
717 81. T. A. Sasani *et al.*, A natural mutator allele shapes mutation spectrum variation in
718 mice. *Nature* **605**, 497-502 (2022).
719 82. B. Xia *et al.*, Widespread Transcriptional Scanning in the Testis Modulates Gene
720 Evolution Rates. *Cell* **180**, 248-262.e221 (2020).
721 83. J. Maynard Smith *et al.*, Developmental Constraints and Evolution. *Q Rev Biol* **60**,
722 265-287 (1985).
723 84. W. Arthur, Developmental drive: an important determinant of the direction of
724 phenotypic evolution. *Evolution and Development* **3**, 271-278 (2001).

725 85. P. Majic, E. Y. Erten, J. L. Payne, The adaptive potential of nonheritable somatic
726 mutations. *The American Naturalist* 10.1086/721766 (2022).
727 86. R. Galupa *et al.*, Enhancer architecture and chromatin accessibility constrain
728 phenotypic space during Drosophila development. *Dev Cell* **58**, 51-62.e54 (2023).
729 87. S. Wright, The roles of mutation, inbreeding, crossbreeding, and selection in
730 evolution. 355-366 (1932).
731 88. R. Dawkins, *The selfish gene* (Oxford University Press, Oxford, 1976), pp. xii, 224
732 p.
733 89. N. M. Foley *et al.*, A genomic timescale for placental mammal evolution. *Science*
734 **380** (2023).
735 90. R. Sender, S. Fuchs, R. Milo, Revised Estimates for the Number of Human and
736 Bacteria Cells in the Body. *PLOS Biology* **14** (2016).
737 91. B. Milholland *et al.*, Differences between germline and somatic mutation rates in
738 humans and mice. *Nat Commun* **8** (2017).
739 92. X. Wang, "Diversity: Who Is Who in the Dog Family" in Dogs: Their Fossil
740 Relatives and Evolutionary History. (Columbia University Press, 2008),
741 10.7312/wang13528-004, pp. 23-68.
742 93. S. J. Rossiter *et al.*, Phylogenomic Resolution of the Cetacean Tree of Life Using
743 Target Sequence Capture. *Systematic Biology* **69**, 479-501 (2020).
744 94. A. Hassanin, E. J. P. Douzery, J. Thorne, Molecular and Morphological
745 Phylogenies of Ruminantia and the Alternative Position of the Moschidae.
746 *Systematic Biology* **52**, 206-228 (2003).
747 95. W. E. Johnson *et al.*, The Late Miocene Radiation of Modern Felidae: A Genetic
748 Assessment. *Science* **311**, 73-77 (2006).
749 96. C. J. Law, G. J. Slater, R. S. Mehta, Lineage Diversity and Size Disparity in
750 Musteloidea: Testing Patterns of Adaptive Radiation Using Molecular and Fossil-
751 Based Methods. *Systematic Biology* **67**, 127-144 (2018).
752 97. C. Gilbert, A. Ropiquet, A. Hassanin, Mitochondrial and nuclear phylogenies of
753 Cervidae (Mammalia, Ruminantia): Systematics, morphology, and biogeography.
754 *Molecular Phylogenetics and Evolution* **40**, 101-117 (2006).

Figures and Tables

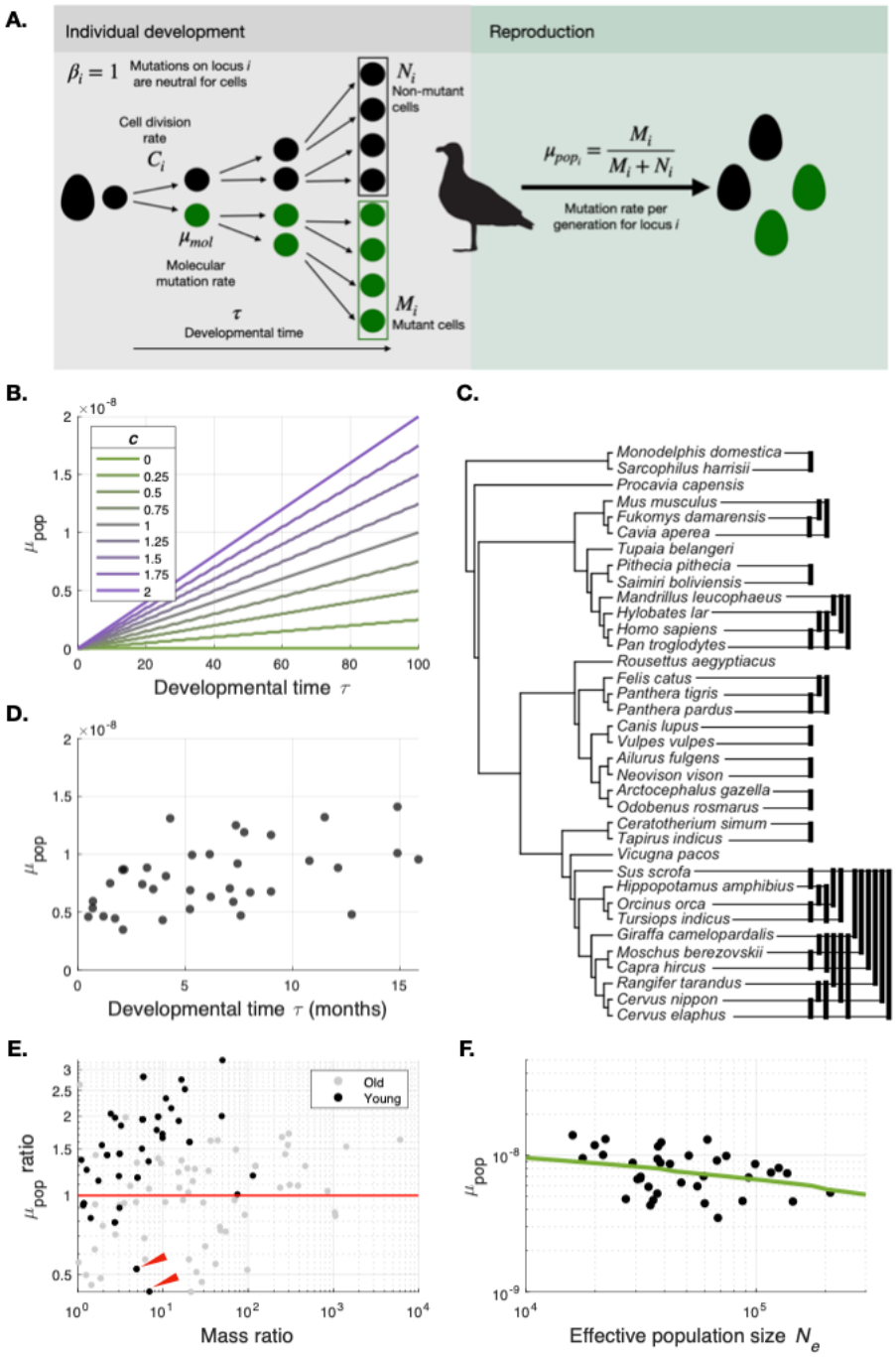

Figure 1. Changes in developmental parameters can causally explain diversification of mutation rates. (A) Illustrated summary of the core model consisting of an individual developmental phase and a reproductive phase. In the developmental phase a lineage starting from a single cell goes through successive cell divisions at a rate *C* over a developmental time τ. During development, mutations can

762 occur at a rate μ_{mol}. Cell proliferation could be affected by the fitness effect of mutations on cells β.
763 For β = 1 mutations are neutral. At the end of development, during the reproductive phase, the
764 fraction of germline-capable cells that carry mutations define the rate at which new alleles are added
765 to the gene pool μ_{pop}. (B) Population-level mutation rate μ_{pop} at a single locus *i* as a function of τ. Each
766 curve represents a different value of *C.* μ_{mol} was held constant at a value of $1x10^{-10}$ mutations per cell
767 division, approximating empirical estimates for human and mouse (91). (C) Phylogeny of mammals for
768 which estimations for μ_{pop} are available (16). Black bars indicate recently diverged species pairs for
769 which body size and μ_{pop} were considered. (D) μ_{pop} for each mammalian species in (C) as a function of
770 their gestation time, a proxy for τ. (E) Ratio of the μ_{pop} of species pairs as a function of the ratio of the
771 mass of species pairs. Black dots indicate branchings younger than 65 my, while gray dots represent
772 older branchings. Notice how, for the vast majority of comparisons between younger branches μ_{pop}
773 ratios are above 1 (red line), which means that larger clades tend to have higher mutation rates, as
774 predicted by our model. Red arrowheads indicate the species pairs corresponding to the tiger
775 (*Panthera tigris*) and leopard (*Panthera pardus*) and goat (*Capra hircus*) and dwarf musk deer (*Moschus*
776 *berezovskii*) (F) Datapoints represent the expected relationship between the predicted μ_{pop} of each of
777 the studied mammalian species and their effective population size N_e based on their body mass
778 (Methods). The green line represents the prediction of this relationship based on our developmental
779 model for μ_{pop}.

780

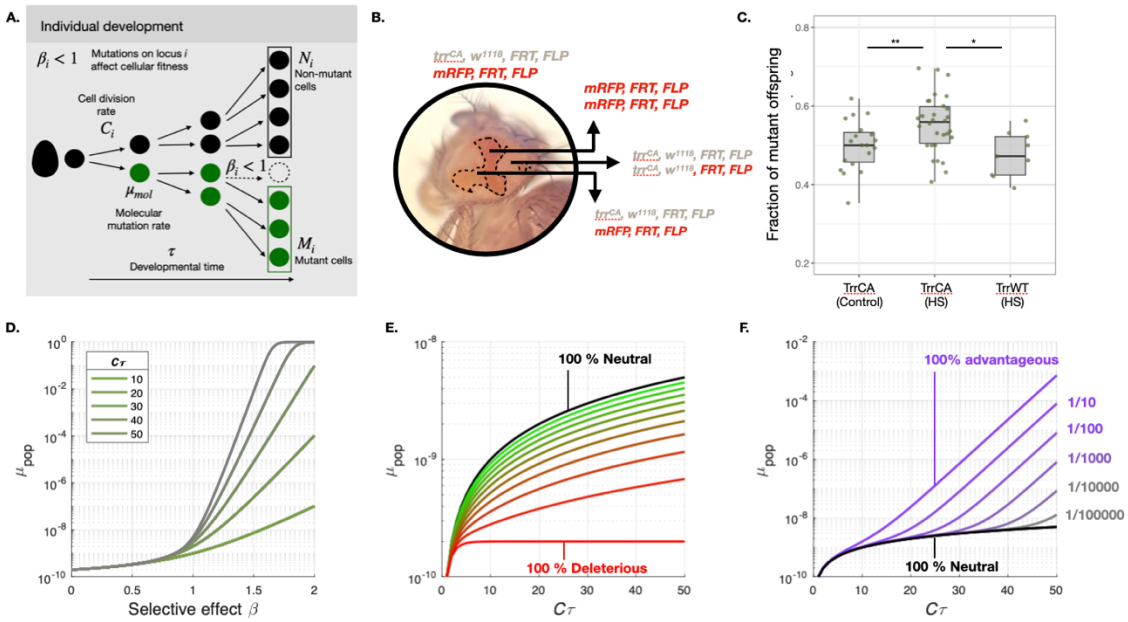

Figure 2. The impact of mutations on cell fitness during development can repercuss on mutation rates. (A) In the model introduced in Fig. 1A, when $\beta \neq 1$, mutations can affect the total number of mutated cells at the end of development *M*. (B) Induced mitotic recombination can generate mosaic organisms with cells with different genotypes. The shown specimen corresponds to a female *Drosophila melanogaster* on which mosaicism can be easily observed in the eyes. Red, white, and orange patches represent each of the possible genotypes thanks to the w^{1118} allele. (C) Fraction of offspring carrying the mRFP(-) allele from crossing a female of interest with a w^{1118} male. TrrCA refers to females of the trr^{CA},w^{1118} genotype, while TrrWT refers to the w^{1118} genotype that is wild-type for *trr*. "HS" refers to females that developed from embryos that were heat-shocked, while "Control" females developed from embryos that were not heat-shocked. Each point represents the fraction of offspring from a different mother. * indicates $p < 0.05$, ** indicates $p < 0.005$ using a Wilcoxon test. (D) Population-level mutation rate μ_{pop} as a function of the effect of mutations on the fitness of cells β. Each curve represents a different value of developmental time τ with a constant value for $C = 1$. (E) Population-level mutation rate μ_{pop} as a function of developmental parameters $C\tau$. Each curve represents a different value proportion of neutral or deleterious mutations. (F) Population-level mutation rate μ_{pop} as a function of developmental parameters $C\tau$. Each curve represents a different proportion of mutations that are advantageous for the cell ($\beta = 1.5$) in the context of an otherwise fully neutral sequence.

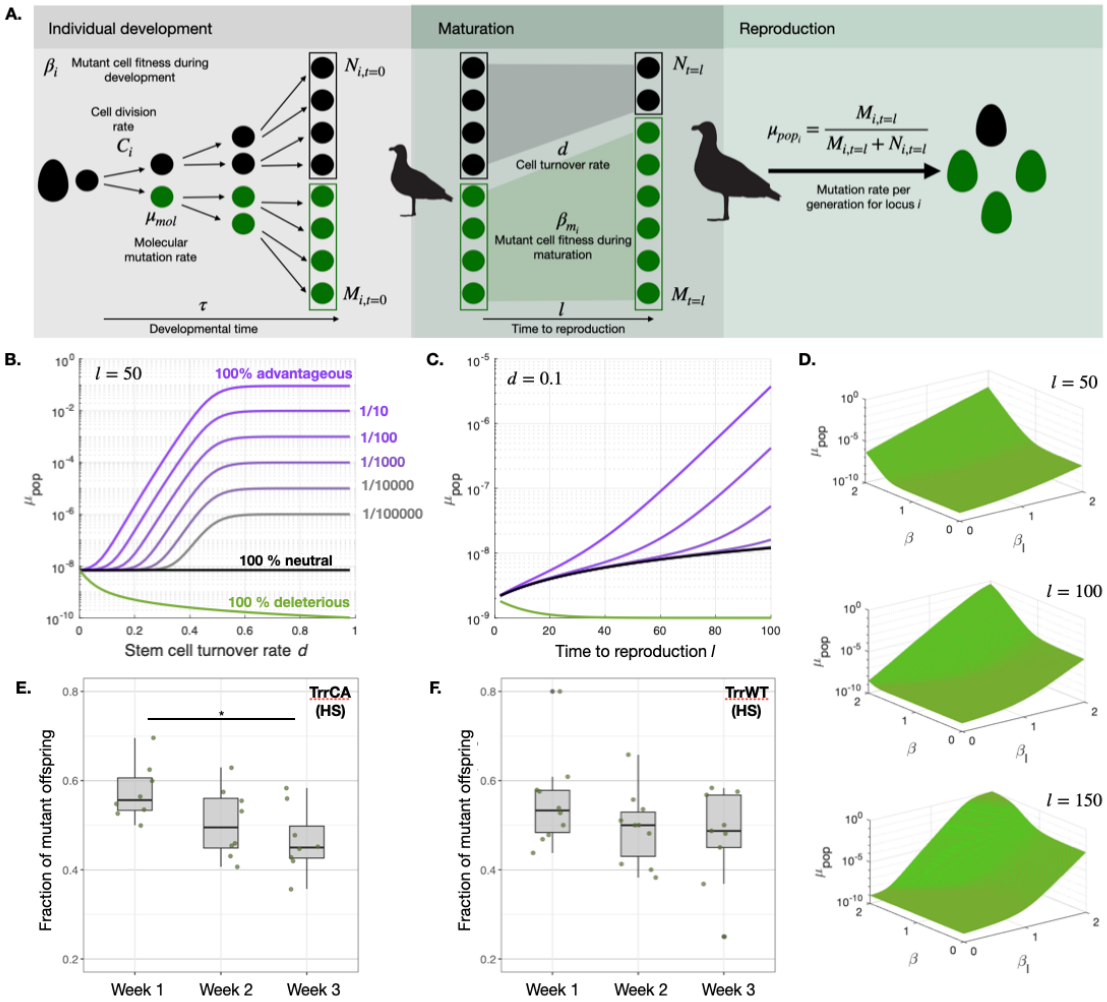

Figure 3. Selection within the germline stem cell niche can also impact mutation rates over an organism's lifetime. (A) Illustrated summary of the model integrating a maturation phase before reproduction. Adding this phase incorporates parameters such as the time to reproduction of an organism *l*, a turnover rate of germline stem cells *d*, and a cellular fitness variable for the stem cell niche β_l. (B) Population-level mutation rate μ_{pop} as a function of the rate of stem cell turnover *d* for a constant generation time of *l = 50*. Each curve represents a different proportion of mutations that are advantageous for the cell ($\beta_l = 1.5$) in the context of an otherwise fully neutral sequence (gray to purple lines), a fully neutral case (black) or a fully deleterious case (green). (C) Population-level mutation rate μ_{pop} as a function of generation time *l* for a constant rate of stem cell turnover *d* = 0.1. The different lines follow the same color code as in (B). (D) μ_{pop} as a function of cellular fitness variable for the stem cell niche β_l for different values of *l* and the fitness effect of mutation on cells during development β. (E and F) Fraction of offspring carrying the mRFP(-) allele from the same set of mothers reproducing at the beginning of weeks one, two or three post-hatching. TrrCA refers to females of the trr^{CA},w^{1118} genotype, while TrrWT refers to the w^{1118} genotype that is wild-type for *trr*. "HS" refers to females that developed from embryos that were heat-shocked. * indicates $p < 0.05$.

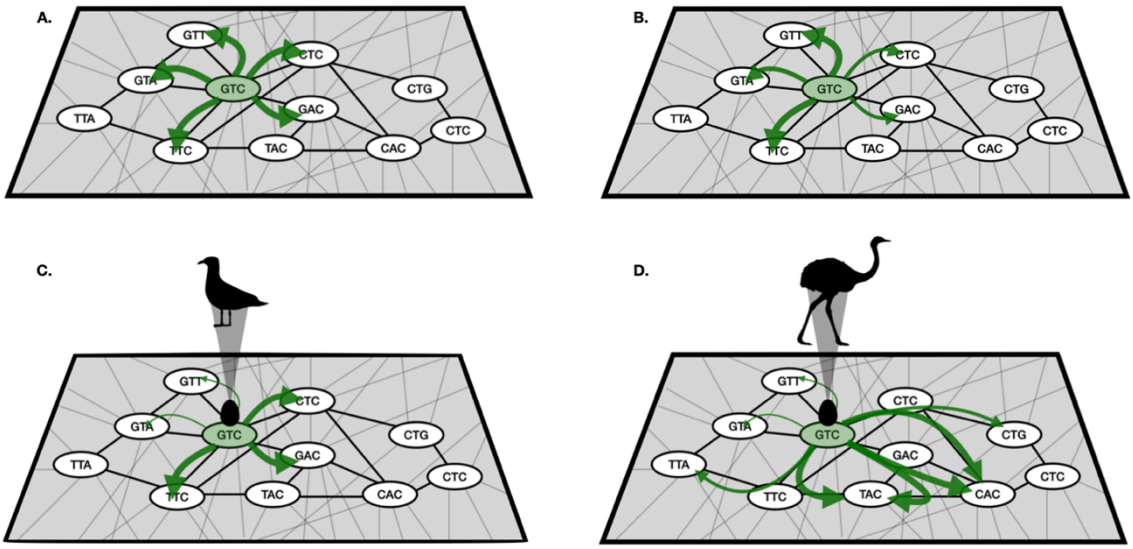

Figure 4. How development can influence the trajectories and pace of genotypic evolution. In a theoretical model of evolution, it could be considered that given a starting genotype, GTC, all mutational steps are equally likely (A). However, if molecular realism is considered there are certain mutations that are more likely than others, as represented by arrows of different thickness going to CTC and GAC. (B). Furthermore, as we argue in this work, development can act as a selective filter for mutations which increases or decreases the likelihood of mutational steps depending on how a mutation affects the cell lineage it belongs to (C). Developmental and life-history differences can also impact how far mutational steps can take an organism. As per our model, larger organisms should be capable of more broadly exploring genotypic spaces within a generation (D).

828 **Supplementary materials**

829 **Table S1. Empirical parameters for 36 mammalian species.**

830 Bergeron et al (2023) estimated the number of de novo mutations in parent-offspring trios of each of
831 the studied species. With those estimations we calculated μ_{pop} as the average of all replicates reported.
832 The mass and τ (gestation time) values were collected from the Encyclopedia of Life (Parr et al 2014).
833 Branch ages representing the estimated divergence time from the closest relative in the phylogeny
834 (Fig. 1C) were gathered from several sources indicated by the superindeces in the Branch Age column:
835 [1](89), [2](92) [3](93) [4](94) [5](95) [6](96) [7](97).

Species	μ_{pop}	Mass (grams)	τ (months)	Branch age (my)
Vicugna pacos	9.44 x10^{-9}	60000	10.79	66[1]
Cavia aperea	8.67 x10^{-9}	442.8	2.07	56[1]
Rousettus aegyptiacus	8.11 x10^{-9}	135.5	4.1	80[1]
Saimiri boliviensis boliviensis	6.90 x10^{-9}	615	5.23	37.3[1]
Felis catus	3.49 x10^{-9}	2884	2.09967	33.9
Pan troglodytes	1.25 x10^{-8}	49896	7.36	7.246[1]
Sarcophilus harrisii	5.95 x10^{-9}	8109.3	0.7	160[1]
Canis lupus familiaris	8.68 x10^{-9}	32183.3	2.16	33[2]
Tursiops truncatus	8.83 x10^{-9}	209791	12.12	19.5[3]
Mandrillus leucophaeus	6.33 x10^{-9}	18250	6.19	37.71[1]
Vulpes vulpes	4.46 x10^{-9}	5603.75	1.73	33[2]
Hylobates lar	7.05 x10^{-9}	5930	7.08	27[1]
Giraffa camelopardalis	1.01 x10^{-8}	932324.5	14.89	45[4]
Capra hircus	5.26 x10^{-9}	61000	5.22	27.8[1]
Hippopotamus amphibius	1.19 x10^{-8}	1417490	7.75	61[1]
Homo sapiens	1.17 x10^{-8}	58540	9	7.246[1]
Procavia capensis	9.20 x10^{-9}	3029.3	7.44	100[1]
Panthera pardus	8.84 x10^{-9}	52038.3	3.22	10[5]
Neovison vison	4.64 x10^{-9}	834.67	1.19	33[6]
Fukomys damarensis	7.41 x10^{-9}	88.5	3	56[1]
Mus musculus	5.35 x10^{-9}	10.1	0.69	66[1]
Moschus berezovskii	1.00 x10^{-8}	12477	6.1413	27.8[1]
Monodelphis domestica	4.60 x10^{-9}	66.5	0.49	160[1]
Orcinus orca	1.41 x10^{-8}	4300000	14.89	19.5[3]
Sus scrofa	4.32 x10^{-9}	86250	3.95	60[1]
Ailurus fulgens	1.31 x10^{-8}	4900	4.3	33[6]
Rangifer tarandus	5.90 x10^{-9}	94744.67	7.24	20.2[7]
Cervus elaphus yarkandensis	6.71 x10^{-9}	165016	8.03	6.8[7]
Ceratotherium simum simum	9.56 x10^{-9}	2591659.5	15.87	61[1]
Pithecia pithecia	9.94 x10^{-9}	1900	5.32	37.3[1]
Arctocephalus gazella	6.78 x10^{-9}	143500	9	33.9[1]
Tupaia chinensis belangeri	7.50 x10^{-9}	200	1.5	77.69[1]
Cervus nippon	4.71 x10^{-9}	74750	7.59	6.8[7]
Tapirus indicus	4.80 x10^{-9}	296250	12.76	61[1]
Panthera tigris	6.99 x10^{-9}	141132	3.51	10[5]
Odobenus rosmarus	1.32 x10^{-8}	825000	11.5	33.9[1]

836

837
838

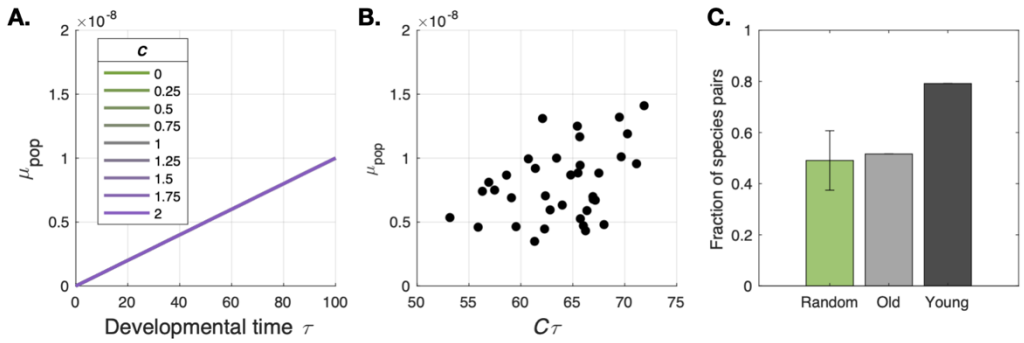

Figure S1. (A) Population-level mutation rate μ_{pop} at a single locus *i* as a function of τ. μ_{mol} was held constant at a value of $1x10^{-10}$ mutations per developmental time unit. Each curve represents a different value of *C*, but they are all collapsed on the same line. (B) μ_{pop} for each mammalian species in Fig. 1C as a function of $C\tau$, which we estimated as the log2 of the number of cells of an organism, measured as the ratio between body mass and the mass of a single cell (Methods). (C) Barplot showing the fraction of species pairs for which the larger of both species also a higher μ_{pop}. The green bar shows the mean fraction of 1000 random permutations of the values with error bars indicating the standard deviation, the gray bar indicates the fraction for species pairs that branched more than 65 mya, while the black bar shows the fraction for recently diverged species pairs.

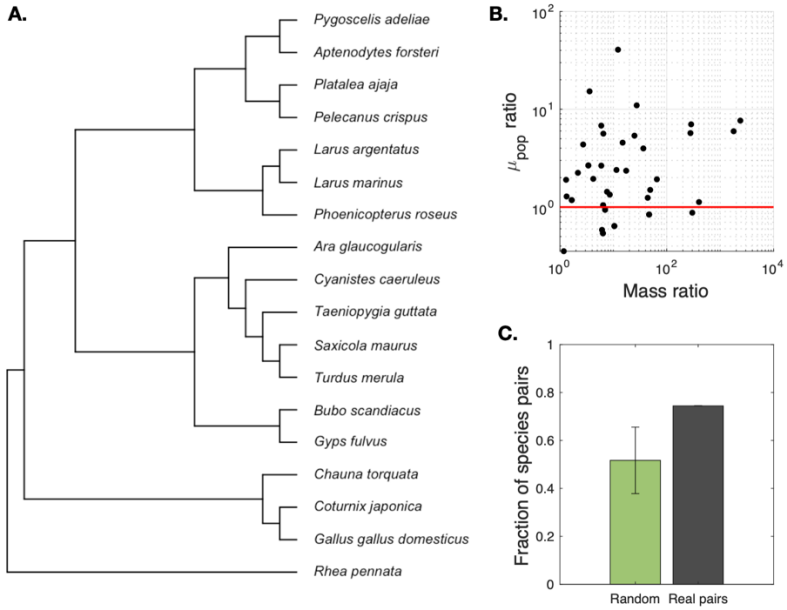

Figure S2. (A) Phylogeny of birds for which estimations for μ_{pop} are available (16). (B) Ratio of the μ_{pop} of species pairs as a function of the ratio of the mass of species pairs. Notice how, for the vast majority of comparisons between younger branches μ_{pop} ratios are above 1 (red line), which means that larger clades tend to have higher mutation rates, as predicted by our model. (C) Barplot showing the fraction of species pairs for which the larger of both species also a higher μ_{pop}. The green bar shows the mean fraction of 1000 random permutations of the values with error bars indicating the standard deviation, while the black bar shows the fraction for all considered empirical species pairs.

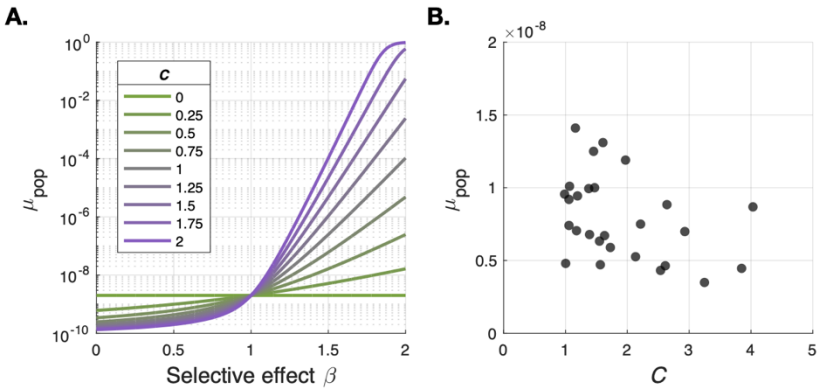

Figure S3. (A) Population-level mutation rate μ_{pop} at a single locus *i* as a function of β_i for τ = 20. μ_{mol} was held constant at a value of 1×10^{-10} mutations per developmental time unit. Each curve represents a different value of *C*. (B) μ_{pop} for each mammalian species in Table S1 for which neonate mass was available as a function of an estimated *C* (Methods).